ARID ZONE JOURNAL OF ENGINEERING, TECHNOLOGY & ENVIRONMENT
AZOJETE December 2023. Vol. 19(4):837-846
Published by the Faculty of Engineering, University of Maiduguri, Maiduguri, Nigeria.
Print ISSN: 1596-2490, Electronic ISSN: 2545-5818
www.azojete.com.ng

IMPACT OF ACID LEACHING ON UPGRADING INDIGENOUS LOW-GRADE CHROMITE ORE FOR IRON AND STEEL PLANT DEVELOPMENT

K. Ayinla[1,3]*, A. A. Baba[1], R. T. Oyewumi-Musa[2], B. C. Tripathy[3], G. A. Anafi[4], R. K. Dwari[3]

[1]*Department of Industrial Chemistry, University of Ilorin, P.M.B. 1515, Ilorin-240003, Nigeria.*
[2]*Department of Chemical and Geological Sciences, Al-Hikmah University, Ilorin, P.M.B. 1501, Nigeria.*
[3]*CSIR - Institute of Minerals and Materials Technology, Bhubaneswar-751013, India.*
[4]*Department of Science Laboratory Technology, Kwara State Polytechnic, Ilorin, Nigeria*

**Corresponding author's email address: ayinla.ik@unilorin.edu.ng*

ARTICLE INFORMATION

Submitted 11 May, 2023
Revised 27 Sept, 2023
Accepted 19 Oct, 2023

Keywords:
Aluminium
Chromite
Evaluation
Iron
Kinetics
purification

ABSTRACT

Low-grade chromite concentrate from the Tunga Kaduka Benue trough region of north-eastern Nigeria is contaminated with iron and aluminium impurities. To transform it into useful material, such impuririties must be removed for it to be useful for the production of special steel and ferrochrome alloys. Consequently, in this study, a Nigerian chromite was treated by hydrochloric acid (HCl) solution. The influence of leaching duration, acid concentration, reaction temperature, and particle size on the extent of impurities dissolution was determined. From the results obtained, the dissolution of iron and aluminium increases with increasing leaching time, HCl concentration, reaction temperature, and decreasing particle size. Under these conditions, the highest recovery of iron and aluminium was obtained to be 95.54 and 82.51%, respectively. The dissolution kinetics of iron and aluminium was evaluated by shrinking core models. The finding reveals that diffusion through the fluid was the leaching kinetics rate-controlling step of iron and aluminium. The activation energy was found to be 25.33 kJ/mol for iron and 18.42 kJ/mol for aluminium. The residual samples at optimal conditions as analyzed by X-ray powder diffraction and scanning electron microscopy were found to

1.0 Introduction

While Chromium is naturally present in many ores, its economically viable form is chromite. Chromite ore is inert and insoluble in water and some mineral acids while in spinel form (Muthy et al., 2011). The spinel is the main mineral phase of the chromite ore with a composition of AB_2O_4, where the divalent cation A can be Fe^{2+} or Mg^{2+}, and the trivalent cation B can be Fe^{3+}, Cr^{3+}, or Al^{3+}(Atalay and Ozhayoghu, 1989; Atalay and Ozhayoghu, 1989). Consequently, the composition made Chromite ore a complex mineral with an admixture of magnesium, iron, aluminium, and chromium in varying proportions depending on the deposit. Iron can be replaced by magnesium and similarly, chromium by ferric iron or aluminium in the spinel structure to improves Cr:Fe ratio in chromite (Kamolpomwijit et al., 2007). This is a factor that would determine chromite quality for various industrial applications.

The major commercial chromite ore and concentrates-producing countries are South Africa, Zimbabwe, India, and Kazakhstan. These countries represent 90% of world production as a whole and Nigeria and others cover the remaining 10% (Kamari et al., 2001). South Africa has reserves of about 3.1 billion tonnes, making the country a leading producer of chromite. This is followed by Zimbabwe with reserves of about 140 million tonnes and resources of 1 billion

tonnes (Morimoto et al., 1989; Cicek et al.,1998; Cicek et al.,2000; Ji, 2012). Nigeria's output is from *podiform* bodies on the Benue trough of the Zamfara state with reserves put at 65 million tonnes and further resources of 97 million tonnes which are yet to be mined for further industrial applications (Abubakre et al., 2007).

Pure metallic chromium is difficult to produce because it is readily contaminated by many other elements. Therefore, a large quantity of raw chromite ore needs to be mined and beneficiated in various chrome ore beneficiation plants throughout the world to cater for the customized needs of various ferroalloy plant industries (Zhang et al., 1989). The main purpose of the beneficiating process is to render the ore concentrate physically and chemically suitable for subsequent treatments which depend on the mineral characteristics of the ore deposits, gangue mineral assemblage, and the degree of dissemination of constituent minerals (Tinjum et al., 2008; Wazne et al., 2008; Meegado et al., 1996; Atalay et al., 1981).

To cater for a possible menace that can be posed by the tailing disposal process, many alternate methods have been proposed. The research works carried out by Amer and Ibrahim (1986) on hydrometallurgical processing of low-grade chromite ore from Barramiya, Egypt, by oxidative leaching in an autoclave reveals that, at a short processing time of 25 minutes, 90% of chromium in the form of chromate was achieved in only one leaching stage. In addition, some early papers examine the liquid-phase oxidation (LPO) procedure in treating chromite ore tailings utilizing molten NaOH-NaNO3 medium or highly concentrated KOH-KNO3 aqueous solution under oxidative circumstances with air, oxygen, or nitrate as the oxidant. (Banerjee et al., 2005; Hundley et al., 1985; Kashiwase et al., 1974). The yield of chromium extraction in this technique has completely addressed the aforementioned threat of tailing disposal with zero waste.

It is critical to design an eco-friendly and low energy cost beneficiation mechanism for treating Nigerian origin chromite ore in order to serve as an alternative to other beneficiation processes revealed by literature and to solve the problem associated with energy consumption and equipment requirements for successful gravity separation and flotation process. The goal of this study is to look into the effect of various parameters on the kinetics of chromite ore dissolution in HCl solution. This aims to examine the dissolution mechanism and develop an empirical equation linking the rate constant of ore leaching to particle size, system temperature, and HCl concentration for the purpose of scaling up and process design for the iron and steel industries.

2.0 Materials and Methods

2.1 Materials

The chromite sample used in this study was sourced from Tunga Kaduka (12°06′30″N 5°56′00″E), Anka Local Government of Zamfara state, north-western Nigeria. The ore was crushed and pulverized into fine particles with the aid of a laboratory crusher and mill; and sieved into four different particle sizes < 78 µm, 110 µm, 218 µm, and 358 µm using the ASTM standard sieves. Hydrochloric acid used was of analytical grade. All the solutions with specified concentrations were prepared with distilled water.

2.2 Mechanical activation of chromite

A twin-bowl INSMART planetary ball mill (Model PBM-07) with an overall capacity of 500 mL and a useful capacity of 250 mL was used for mechanical activation work on the chromite ore. This was carried out at 300 r/min using 10 mm diameter stainless steel balls keeping the ball-to-powder mass ratio at 10:1. Milling was carried out for the duration of 1 h (Kamari et al., 1999).

Corresponding author's e-mail address: ayinla.ik@unilorin.edu.ng

2.3 Experimental procedures

The leaching experiments were performed in a glass 250-mL flask equipped with a magnetic stirrer using an agitation speed of 200 rpm and a reflux condenser to prevent evaporation loss, which was bathed in a water bath. Chromite (2 g) was reacted with different concentrations of hydrochloric acid (0.1–2.0 mol/L), with different hydrochloric acid/chromite mass ratios (3:1–7:1 mL/g), different leaching times (15–120 min), and different leaching temperatures (28, 30, 40, 60 and 80 °C). After the acid leaching, the mixture was filtered through 0.5-µm pore size white filter paper using a pressure filtration unit and washed to separate the leached residue and the solution. The $Mg^{2+,}$ $Fe^{3+,}$ and Al^{3+} contents in the solutions were determined using atomic Absorption Spectroscopy (AAS) and a flame photometer. The residue at optimal conditions was analyzed by X-ray Fluorescence (XRF), scanning electron micrograph (SEM), and X-ray diffraction (Kamari et al.,2001).

3.0 Results and Discussion

3.1 Ore Characterization

The X-ray patterns of the milled ore at two different particle sizes (75 µm and 210 µm) are illustrated in Figure 1.

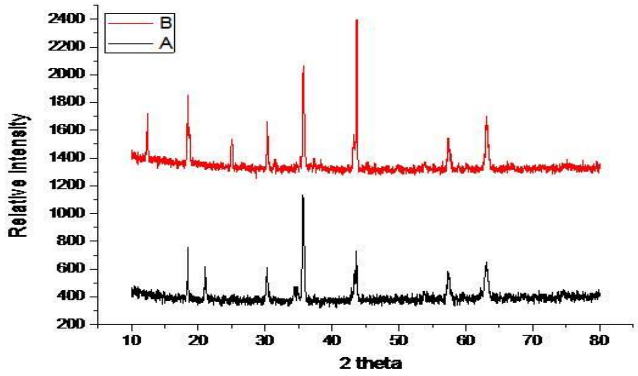

Figure 1: XRD spectra of raw grounded and harmer mill chromite ore to size (A) 210 µm (B) 75 µm.

The XRD pattern of the 210 µm sample (Figure 1(A)) indicates that the ore is primarily comprised of chromite ($FeCr_2O_3$) {JCPDS No. 32-2007}, hematite (Fe_2O_3) {JCPDS No. 21 - 0034}, and alumina (Al_2O_3) {JCPDS No. 01- 1338} phases. However, after 60 minutes of high energy milling (Figure 1(B)), the corresponding phases of quartz (SiO_2), ilmenite), rutile (TiO_2), and bixbyite (Mn_2O_3) were slightly broadened and their intensity decreased due to the refinement of crystalline grains and the accumulation of lattice distortion caused by ball impact and collision. (Than et al., 1970; Xu et al., 2005). The elemental composition by EDS of raw chromite ore is presented in Fig. 2. The chemical composition of the raw chromite powder examined by EDXRF gave 38.34% Cr, 33.80% Fe, 19.70% Al, 13.84% Si, 3.69% Mg, 0.14% Mn, and 0.55% Ti by weight. Also, the EDS spectrum (Figure 2) was in support of EDXRF revealing Cr_2O_3 (20.3%), Fe_2O_3 (6.39%), SiO_2 (4.13%), and Al_2O_3 (6.67%) as major constituents present in the studied ore.

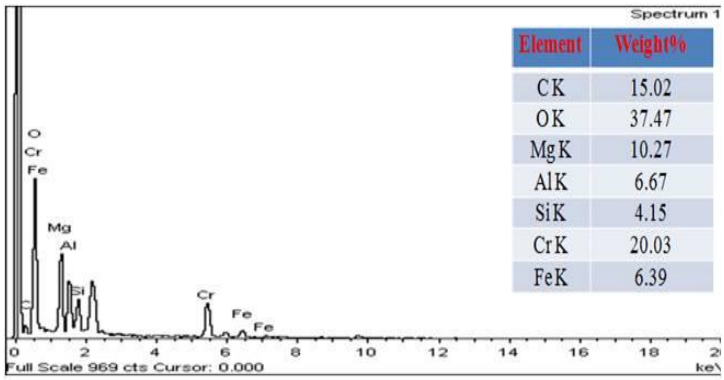

Figure 2: EDS diffractogram of raw chromite powder

From the SEM result (Figure 3A), a distinct light grey region (A) and dark grey region (B) denote the presence of manganese and ferro silicate compounds while Figure 3B&C indicate distinctive textural features in the raw ore.

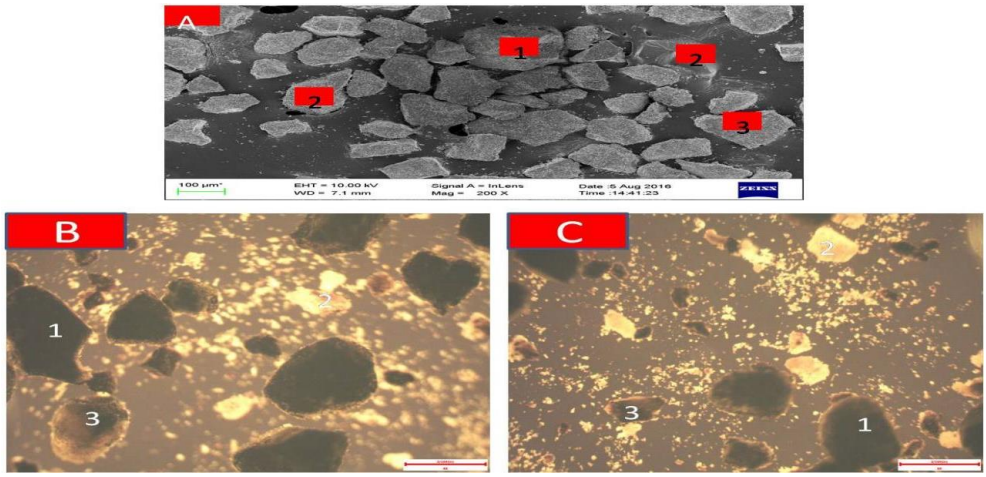

Figure 3: The microstructural morphology of the chromite powder (a) SEM image
(b) Photomicrograph at 310 µm (scale: 2/100 nm 4X)
(c) Photomicrograph at 78 µm (scale: 2/100 nm 4X)

The black cuboids' mineral phase (1) is attributed to chromite ($FeCr_2O_4$), complemented with the large coal brown region (2) which is attributed to thermally stable alumina and manganese oxide, indicating bixbyite (Mn_2O_3). Also, an admixture of iron and other trace impurities in the form of haematite (Fe_2O_3) is present in the brownish region marked as (3) while the predominant associated gauges are identified as siliceous compound (SiO_2) can be found underneath (Vandar et al., 1994; Zanello and Raspi, 1977).

3.2 Extraction results

3.2.1 Effect of leaching time

Based on the mineralogical analysis results, the effect of leaching time was first investigated and the details are summarized in Figure 4.

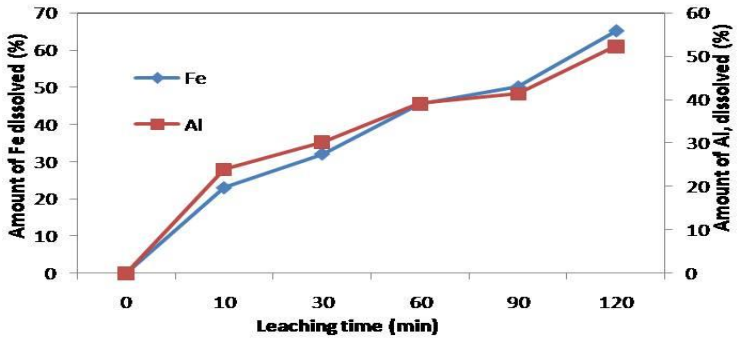

Figure 4: Influence of leaching time on Fe and Al dissolution from chromite ore

As shown in Figure 4, the effect of the reaction time on the leaching efficiency of Fe and Al atacid concentration of 0.5 mol/L, and 55°C.The leaching efficiency of Fe and Al into solution increases as leaching time increases. This could be related to the creation of water-soluble Al and Fe chlorides. When the leaching time was 1 h, the leaching efficiency of Fe and Al was observed to be less than55%. Similarly, when the time was extended to 1.5 h, the leaching efficiency of Fe and Al further increased to 60%; and more than 68% of Fe and Al can be leached out after 2 h. Also, Figure 3 shows that the dissolution rates of Fe and Al are very close and reach an apparent steady-state within 2 h. Therefore, 2 h was agreed to be the optimum duration for the leaching of Fe and Al.

3.2.2 Effect of HCl concentration

The effect of acid concentrations on the leaching are shown in Figure 5.

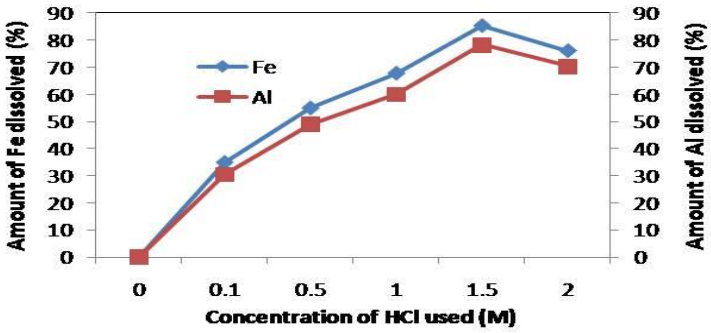

Figure 5: Influence of hydrochloric acid concentration on Fe and Al dissolution from chromite ore

It can be seen that the acid concentration has a significant impact on the leaching efficiency of Fe and Al, whose leaching efficiency was raised from 35 to 85% and 30 to 74% when the acid concentration of HCl was varied from 1.0 mol/L to 2.0 mol/L respectively. This is due to the acid concentration effect on increasing the H^+ activity that results in further dissolution of Al and Fe impurity (Sun et al., 2007). The leaching efficiency reached the maximum value at the acid concentration of 1.5 mol/L. The reason for this may be due to the chromite structure collapsing at this concentration or Fe^{2+} and Al^{3+} species blocking H^+ diffusion (Wang et al., 2008).

3.2.3 Effect of leaching temperature

Figure 6 shows the effect of reaction temperatures on the leaching efficiency of Fe and Al at a hydrochloric acid concentration of 1.5mol/L, time of 2 h and hydrochloric acid-to-chromite ratio of 4 mL/g. As expected, the leaching efficiency of Fe and Al increases with rising temperatures and the leaching efficiency of Fe and Al was up to 95.8% and 84.9% at 80 °C. However, the temperatures that continue to rise is advantageous to the formation of jarosite because of the presence of Fe, which could lead to a poor leaching efficiency of Al (Ayinla et al., 2019). In addition, Al may also be incorporated into the leached residue as a result of the precipitation of alunite and therefore cause a fall in the purity of silica gel (Baba et al., 2013). Thus, the optimized condition of the leaching temperature is 80 °C.

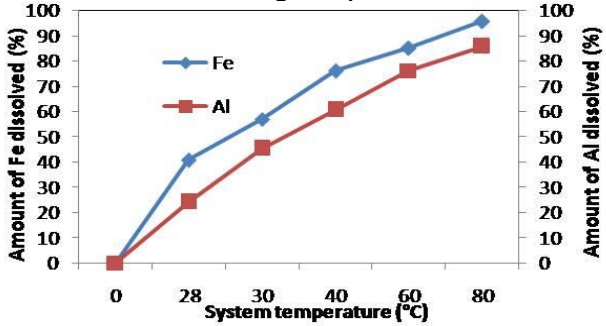

Figure 6: Influence of leaching temperature on Fe and Al dissolution from chromite ore

3.2.4 Effect of particle size

The influence of particle size (78-358µm) was also tested. A particle size value corresponds to 100% of the particles below that size. The results showed that the particle size affected the iron and aluminium extractions (Figure 7)

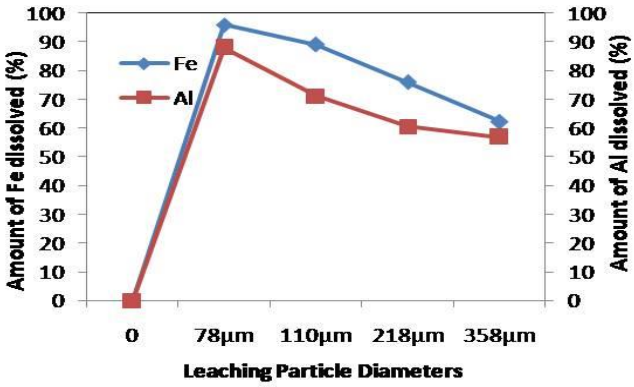

Figure 7: Influence of leaching particle diameter on Fe and Al dissolution from chromite ore

Figure 7 shows that the amounts of extracted iron and aluminium increased when the particle size decreased. In the range of 358-78 µm, these trends became steeper because of the effect of increased specific surface area. The results showed that grinding was beneficial to extractions of the metal values because more grinding increased the iron and aluminium extractions. However, this technique has technical and economic restrictions. When the chromite ore samples were ground to 78 µm, the extracted iron and aluminium were about 95% and 89%, respectively.

3.3 Kinetics analysis

The reactions occurring during the leaching process are typically heterogeneous (Ekmekyapar et al., 2012) and the relevant kinetics follow the shrinking core model which was described by Lid-dell in detail (Liddell, 2005). The following expressions can be used to describe the leaching process kinetics (Levenspiel, 1999; Meegoda, 1999):

For diffusion control through the fluid film:

$$1 - (1 - \alpha)^{2/3} = kt \quad (1)$$

For solid product diffusion control:

$$1 - 3(1 - \alpha)^{2/3} + 2(1 - \alpha) = kt \quad (2)$$

For surface chemical reaction control:

$$1 - (1 - \alpha)^{1/3} = kt \quad (3)$$

where αis the fractional conversion of iron and aluminium, *t* is the reaction time (min) and *k* is the apparent rate constant(min−1). The overall rate of dissolution is controlled by the slowest of these sequential steps. Values of Eqs. (1) – (2) versus the reaction time were plotted to determine the kinetic parameters and leaching rate controlling step comparing the R^2 values to ascertain the most fitted. The results are shown in Table 1.

Table 1: Apparent rate constant (*k*) for kinetic models and correlation coefficient values

	Temperature °C	Diffusion through the product layer		Surface chemical reaction	
		k(min^{-1})	R^2	k(min^{-1})	R^2
Iron	28	0.0029	0.9823	0.0011	0.7625
	30	0.0027	0.9866	0.0016	0.8854
	40	0.0035	0.9913	0.0020	0.8812
	60	0.0045	0.9813	0.0025	0.7895
	80	0.0046	0.9925	0.0028	0.8814

	28	0.0020	0.9856	0.0010	0.7120
	30	0.0025	0.9830	0.0014	0.8812
Aluminium	40	0.0030	0.9825	0.0019	0.8945
	60	0.0035	0.9914	0.0022	0.8350
	80	0.0038	0.9923	0.0025	0.8912

It is obvious from Table 1 that the highest R^2 values were obtained for the diffusion through the product layer. Additionally, in leaching processes, the dissolution ratio directly depends on the activation energy, which can be calculated based on the Arrhenius equation ($k = A \times e^{-Ea/R \times T}$). Based on the Arrhenius activation energy theory, the Arrhenius equation was plotted as ln (k) vs. ($1/T$) for each temperature and the activation energies were calculated from the slopes of straight lines (Figure 8A &B).

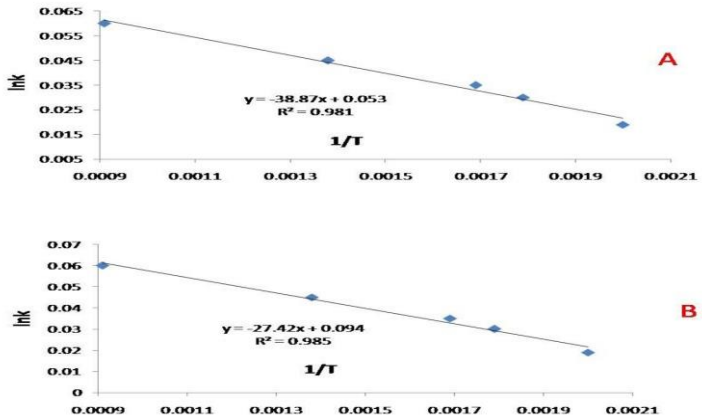

Figure 8: Plot of lnk versus 1/T for activation energy calculation: (A) graph for iron removal (B) graph for aluminium removal

Where the slope is $-Ea/R$. The values of activation energies (Ea) and frequency factors (A, min^{-1}) calculated from Arrhenius plot are 25.33 kJ/mol for iron and 18.42 kJ/mol for aluminium. It has been previously stated that the typical activation energy for a chemically controlled process is greater than 40 kJ/mol, while the activation energy of a diffusion-controlled process is usually below 40 kJ/mol (Ekmekyapar et al., 2012). From the results obtained, it can be concluded that the leaching process of iron and aluminium from low-grade chromite ore of Nigerian origin using hydrochloric acid is controlled by the diffusion process. Consequently, the equations representing the kinetics of the leaching process of iron and aluminium can be expressed according to Eqs. (7) and (8), respectively.

$$1-3(1-\alpha)^{2/3} + 2(1-\alpha) = 0.7272 \times e^{-28.35/8.314T} \times t \quad (4)$$

$$1 - 3(1-\alpha)^{2/3} + 2(1-\alpha) = 0.9686 \times e^{-13.92/8.314T} \times t \quad (5)$$

3.4 Residue analysis

XRF analysis was used for the elemental analysis of chromite ore concentrate after leaching (Table 2). The amount of Fe and Al drastically decreases which gives rise to an increase in the value of Cr in the chromite ore (54.46 %). An unexpected increase in Si and Ti content was also observed during the leaching process. This could be due to un-dissolve silica-containing minerals which are insoluble in the acidic solution.

Table 2: XRF analysis result of chromite or before and after acid leaching

Elemental composition	Before leaching (%)	After leaching (%)
Cr	38.34	59.22
Fe	33.80	5.76
Al	19.20	6.40
Si	13.84	23.07

Mg	3.69	3.31
Mn	0.14	1.19
Ti	0.55	1.07

The morphologies of the leaching residues obtained under optimum conditions were analyzed by using the XRD method (Figure 9A-C).

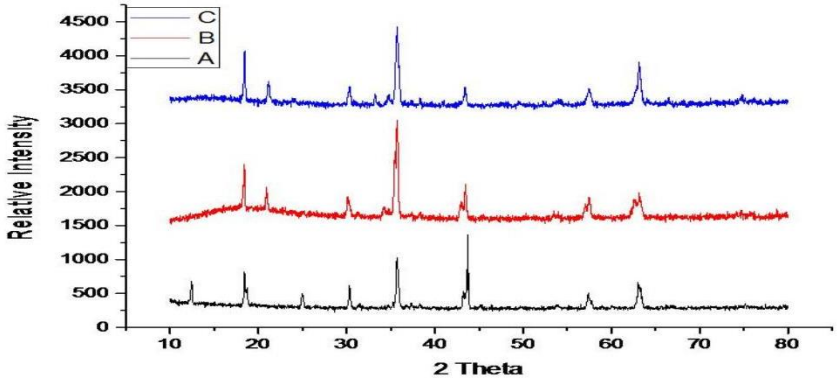

Figure 9: XRD spectra of leach residues at optimum conditions (a) at 30 min (b) 60 min(c) 120 min

In the diffractogram of leached residue (Figure 9c)), the presence of phases Cr_2O_3 and $MgCrO_4$ are indicated. The presence of un-reacted SiO_2 could not be identified in the diffractogram, which may be due to the smaller amount compared with the other phases or their peak intensity might be reduced due to the formation of new phases with somehow bigger grain sizes. However, other peaks as indicated by the XRD pattern of the final acid leaching residue comprised of TiO_2 and $FeTiO_3$ phases which did not react during acid leaching. To examine the microstructure of the partially reacted chromite ore, the cross-section of the leaching residue was polished and examined using SEM. The SEM of acid-leached residue after drying along with water-washed residues after drying are shown Figure 10a-b.

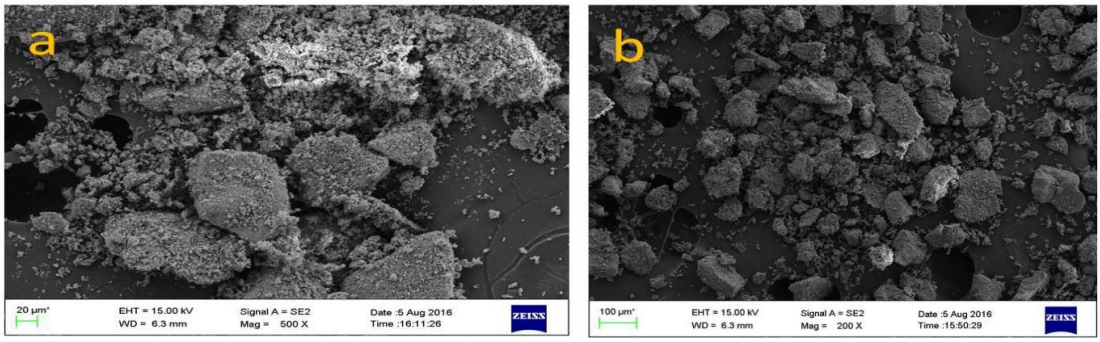

Figure 10: SEM images of leached residues at optimum leaching conditions

It is observed that smooth and nearly cubical grains (Figure 3(a)) of milled chromite ore are completely transformed into porous and nodular clusters of particles after leaching (Figure 10(a)). During the water treatment of the leached residues, excess acid is removed along with water-soluble titanates/ferrates causing the agglomerated form to collapse and particles become mostly free (Figure 10(b)). Final acid leaching residue mostly contains unreacted chromite, silica and rutile which were not converted during acid leaching.

4.0 Conclusions

In this study, acid leaching of Nigerian chromite ore by hydrochloric acid for purification of low-grade chromite ore as potential raw material for the production of special steel and ferrochrome alloys. In the range of studied parameters, the most suitable conditions for the leaching process of iron and aluminium attained at temperature 80°C, 1.5 M HCl, L/S ratio = 20 g/L and 78 µm particle size dissolution. Under these conditions, it was found that iron

leaching recovery of 95.54 % with a aluminium leaching recovery of 82.51% could be obtained. The dissolution kinetics of iron and aluminium support diffusion as the rate-controlling step. The activation energies were determined to be 25.33 and 13.42 kJ/mol for the leaching of iron and aluminium, respectively. The residue evaluation was carried out using XRF, XRD and SEM respectively, the obtained result clearly showed the presence of Cr_2O_3, $MgCrO_4$ and SiO_2 as the major mineral phase.

References

Abubakre, OK., Muriana, RA. and Nwokike, PN. 2007. Characterization and beneficiation of Anka chromite ore using magnetic separation process. Journal of Minerals & Materials Characterization & Engineering, 6 (2): 143–150.

Amer, M. and Ibrahim, IA. 1996. Leaching of a low-grade Egyptian chromite ore. Hydrometallurgy, 43 (1–3): 307–316.

Atalay, MU., Ozbayoglu, G. and Dogan, MZ. 1989. Mechanism of collector adsorption in chromite flotation. In: Aytekin, Y. (Ed.), Proceedings of II International Mineral Processing Symposium, Izmir, Turkey, pp. 441–449.

Atalay, U. and Ozbayoglu, G. 1992. Beneficiation and agglomeration of chromite–its application in Turkey. Mineral Processing and Extractive Metallurgy Review, 9:185–194.

Ayinla, IK., Baba, AA., Padhy, SK., Adio, O., Odeleye, KA. and Tripathy, BC. 2019. Synthesis and Characterization of Pure Silica Powder from a K-Feldspar Silicate Ore for Industrial Value Addition. Faculty Science University Ankara Series B, 61 (1-2): 69-87.

Baba, AA., Ayinla, IK., Adekola, FA., Bale, RB., Ghosh, MK., Alabi, AGF., Sheik, AR. and Folorunso, IO. 2013. Hydrometallurgical application for treating a Nigerian chalcopyrite ore in chloride medium: Part I. Dissolution kinetics assessment. International Journal of Minerals; Metallurgy and Materials, 20(11): 1-8.

Banerjee, TH., Sengupta, AK., Gundewar, TS. and Amanullah, CS. 2005. Proposed modified process flow-sheet for augmenting the throughput capacity of Chrome ore beneficiation plant of M/s TISCO, Sukinda, Orissa. In: International Conference on Mineral Processing Technology MPT-2005., (12-16 December, 2005), Bombay, 623–631.

Cicek, T., Cocen, I. and Birlik, M. 2000. Applicability of multi-gravity separation to kop chromite concentration plant. In: Mineral Processing on the Verge of the 21th Century, (12-16 November 2000) Balkema, Rotterdam. Proceedings of 8th International Mineral Processing Symposium, Antalya, 87–92.

Cicek, T., Cocen, I. and Samani, S. 1998. Gravimetric concentration of fine chromite tailings. In: Innovations in Mineral and Coal Processing, Balkema, Rotterdam. Proceedings of 7th International Mineral Processing Symposium, Istanbul (10-14, December, 1998), pp. 731–736.

Ekmekyapar, A., Aktaş, E., Künkül A. and Demirkıran, N. 2012. Investigation of leaching kinetics of copper from malachite ore in ammonium nitrate solutions. Metallutgical Material Transaction B, 43:764–72.

Hundley, GL., Nilsen, DN. and Siemens, RE. 1985. Extraction of Chromium from domestic chromite by alkali fusion. U.S. Bureau of Mines, Report of Investigations, RI8977. U.S. Bureau of Mines, Pittsburg, U.S.

Ji, Z. 2012 Preparation of trivalent chromium compounds from chromite by acid-leaching technique. Inorganic Chemistry Indices., 44:1–5.

Corresponding author's e-mail address: ayinla.ik@unilorin.edu.ng

Kamolpornwijit, W., Meegoda, JN. and Hu, Z. 2007. Characterization of chromite ore processing residue Practical Periodic Hazard. Toxic Radioactive Waste Management., 11: 234–23.

Kanari, N., Gaballah, I. and Allain E. 1999. A study of chromite carbochlorination kinetics. Metallurgical Material Transaction. 30:577–587.

Kanari, N., Gaballah, I. and Allain, E. 2001. Kinetics of oxychlorination of chromite. I. Effect of temperature. Thermochimica Acta, 371:143–154.

Kashiwase, K., Sato, G., Atumi, T. and Okabe, T. 1974. Appropriate oxidizing conditions of chromite with molten sodium salts. Nippon Kagaku Kaishi., 3: 469–473.

Levenspiel, O. 1999. Chemical reaction engineering. 3rd ed. New York: John Wiley & Sons;.124.

Liddell, KC. 2005. Shrinking core models in hydrometallurgy: what students are not being told about the pseudo-steady approximation. Hydrometallurgy, 79: 62– 68.

Meegoda, JN., Kamolpornwijit, W., Vaccari, DA., Ezeldin, AS., Noval, BA., Mueller, RT. and Santora, S. 1999. Remediation of chromium-contaminated soils: Bench-scale investigation. Pract. Period. Hazard. Toxic Radioactive Waste Managemen, 3: 124–131.

Morimoto, N., Fabries, J., Ferguson, AK., Ginzburg, IV., Ross, M., Seifeit, FA. and Zussman, J. 1989. Nomenclature of pyroxenes. Canadian Mineralogist, 27: 143–156.

Murthy, YR., Tripathy, SK. and Kumar, CR. 2011. Chrome ore beneficiation challenges and opportunities – A review. Minerals Engineering, 24: 375–380.

Sun, Z., Zheng, SL. and Zhang, Y. 2007. Thermodynamics study on the decomposition of chromite with KOH. Acta Metallurgica Sinica (English Letters), 2 (3): 187– 192.

Than, MJ., Walker, RD. and Gubbins, KE. 1970. Diffusion of oxygen and hydrogen in aqueous potassium hydroxide solutions. The Journal of Physical Chemistry, 74 (8): 1747–1751.

Tinjum, JM., Benson, CH. and Edil, TB. 2008. Mobilization of Cr (VI) from chromite ore processing residue through acid treatment. Scientific Total Environment, 391: 13–25.

Vardar, E., Eric, RH. and Letowski, FK. 1994. Acid leaching of chromite. Minerals Engineering, 7 (5–6): 605–617.

Wang, R., Tang, M., Yang, S., Zhagn, W., Tang, C. and He J. 2008. Leaching kinetics of low-grade zinc oxide ore inNH_3–NH_4Cl–H_2O system. Journal of Central South University Technology, 15:679–683.

Wazne, M., Jagupilla, SC., Moon, DH., Christodoulatos, C. and Koutsospyros, A. 2008. Leaching mechanisms of Cr (VI) from chromite ore processing residue Journal of Environmental. Quality, 37: 2125–2134.

Xu, HB., Zhang, Y., Li, ZH., Zheng, S-L., Wang, Z-K., Qi, T. and Li, H-Q. 2006. Development of a new cleaner production process for producing chromic oxide from chromite ore. Journal of Cleaner Production, 14 (2): 211–219.

Zanello, P. and Raspi, G. 1977. Electrooxidation of chromium (III) in alkaline hydroxide solution at a platinum electrode. Analytica Chimica Acta, 88(2): 237–243.

Zhang, Y., Li, ZH., Wang, ZK. and Chen, JY. 1986. Green chemistry and chromium salt industry a new generation of industrial revolution. Chemical Industry Engineering Progress, 10: 172–178.

Corresponding author's e-mail address: ayinla.ik@unilorin.edu.ng